Separation and Purification Technology 275 (2021) 119177

Contents lists available at ScienceDirect

Separation and Purification Technology

journal homepage: www.elsevier.com/locate/seppur

Boron extraction using selective ion exchange resins enables effective magnesium recovery from lithium rich brines with minimal lithium loss

Luiza Bonin [a,e,*], Davy Deduytsche [b], Mariette Wolthers [c], Victoria Flexer [d], Korneel Rabaey [a,e]

[a] Center for Microbial Ecology and Technology (CMET), Faculty of Bioscience Engineering, Ghent University, Coupure Links 653, Ghent 9000, Belgium
[b] Department of Solid State Sciences, CoCooN Group, Ghent University, Krijgslaan 281/S1, 9000 Gent, Belgium
[c] Department of Earth Sciences, Faculty of Geosciences, Utrecht University, the Netherlands
[d] Centro de Investigación y Desarrollo en Materiales Avanzados y Almacenamiento de Energía de Jujuy-CIDMEJu (CONICET-Universidad Nacional de Jujuy), Av. Martijena S/N, Palpalá 4612, Argentina
[e] CAPTURE, Coupure Links 653, Ghent 9000, Belgium

ARTICLE INFO

Keywords:
Water desalination
Sustainable mining
Raw materials
Ion exchange resin
Crystallization

ABSTRACT

Magnesium hydroxide is a commodity chemical, produced in almost pure form from seawater through precipitation. Even though Li brines contain high concentrations of Mg^{2+} cations, the precipitation of $Mg(OH)_2$ from them is not common. Rather it is typically coprecipitated with other salts and becomes a waste. The crystallization of chemical-grade $Mg(OH)_2$ from a Li^+ rich brine that contained 3.1 g/L Mg^{2+} and 1.3 g/L Li^+, was investigated by means of NaOH and CaO addition. Direct precipitation of $Mg(OH)_2$ leads to considerable Li loss and impure crystals due to the brine uptake into the crystal cake. In order to increase the sedimentation rate and decrease the brine loss, a boron extraction step was introduced, which consisted of initial polishing using Amberlite IRA743. It was possible to extract B to below the ICP detection limit from native salt lake brines selectively and regenerate the ion exchangers for repetitive cycles. Upon the extraction of boron, the $Mg(OH)_2$ sedimentation rate, increased while the loss of Li^+ from the brine decreased from 13.7 ± 1.2 to 1.5 ± 0.4%. Precipitation with CaO as an alkalizing agent generated a mixture of crystals and a Li^+ loss between 6.7 ± 0.8 and 3.8 ± 0.7%. When the boron-free brine was alkalized by NaOH, an increase in the degree of crystallinity of $Mg(OH)_2$ crystal structure was verified by XRD and a purity of 95 ± 2% for the solid was obtained. The high water intake in the presence of B was associated with the presence of hydroboracite in intercalation within the brucite. It was expected that, if the hydroboracite was present as an intercalation, this structure would be disrupted more easily by the ultrasound, potentially resulting in a loss of the hydroboracite d-spacings. Concluding, subsequent B and Mg removal steps from Li^+ rich brines result in the production of 95% pure $Mg(OH)_2$ leaving a brine for high purity lithium salt precipitation, thereby bringing a second attractive product from brine processing.

1. Introduction

The lithium-ion battery plays a pivotal role for electrified applications such as electric cars, mobile electronics and power storage. Even if the word “lithium” comes from the Greek word “lithos” meaning stone, over 60% of the global lithium resources are found in salt lake brines, where lithium chloride is accompanied by other salts [1]. While thus far a larger share of lithium is harvested from spodumene hard rock ores, the recovery of lithium from brines needs to bridge the gap between the demand for electric vehicle sales, and the actual level of supply of battery-grade lithium compounds.

While lithium rich brines have a vast availability and the related extraction processes are cost effective when compared to hard-rock or clay mining [2], selective lithium salts recovery from these aqueous solutions containing various other cations (B^+, Na^+, K^+, Ca^{2+}, Mg^{2+}) is challenging, involving high chemical usage and waste production [3]. These brines have total dissolved solids values of no less than 160 g L^{-1}, reaching in some deposits up to 350 g L^{-1}, making their processing particularly challenging due to the extreme salinity values [4]. The first step typically involves solar evaporation of the native brine with the aim

* Corresponding author at: Center for Microbial Ecology and Technology (CMET), Faculty of Bioscience Engineering, Ghent University, Coupure Links 653, Ghent 9000, Belgium.
E-mail address: Luiza.Bonin@ugent.be (L. Bonin).

https://doi.org/10.1016/j.seppur.2021.119177
Received 17 May 2021; Received in revised form 17 June 2021; Accepted 18 June 2021
Available online 23 June 2021

of precipitating a large share of NaCl, the main brine component, and KCl, while concentrating the originally diluted Li^+ cations. This is followed by removal of magnesium, calcium, sulphate and boron using additives, further evaporation, ion exchange polishing prior to the final Li_2CO_3 precipitation [5].

The solar evaporation is not only responsible for high volumes of water loss [3], but also for losses of up to 50% of Li^+ due to the formation of mixed crystals in the ponds (principally lithium carnallite, LiCl. $MgCl_2{\cdot}6H_2O$) [6]. Moreover, a share of valuable Li^+ ions is also trapped upon precipitation of $Mg(OH)_2$ during lime addition. The ionic radii of Mg^{2+} and Li^+ are almost the same, and thus, Mg salts coprecipitate with Li^+ salts, unless Mg^{2+} has previously been fully removed [7]. The extraction of Mg^{2+} without Li loss is therefore necessary for the economically efficient production of high purity lithium salts, independent of the Li^+ extraction method of choice.

Interestingly, magnesium and magnesite are considered critical elements by the European union [8,9]. To precipitate Mg^{2+} from Li^+ rich brines, soda ash (Na_2CO_3) and burnt lime (CaO), are the most used chemicals [5,7]. However, the above mentioned precipitating substances cannot be used to precipitate chemical grade $Mg(OH)_2$ from Li^+ rich brines as they produce a mixture of Mg and Ca hydroxides/carbonates, including many impurities.

Precipitation of chemical grade $Mg(OH)_2$ from Li^+ rich brines could thus far only be achieved by NaOH/KOH addition, or brine electrolysis [7]. However, the use of OH^- as a precipitating agent, creates substantial technological difficulties. $Mg(OH)_2$ tends to form colloids instead of large crystals, settles very slowly and the final sediment traps high volumes of water and thus other salts, including highly valuable Li^+ ions. Ideally, a new process should be able to recover Mg^{2+} as $Mg(OH)_2$ without any Li loss.

Li^+ rich brines generally also contain boron and MgO/$Mg(OH)_2$ have been reported to be very effective in removing boron from water by adsorption [10,11]. Thus, a key question is whether the boron that is naturally present in Li brines also associates strongly with the $Mg(OH)_2$ crystals and whether it influences the water trapping by $Mg(OH)_2$ precipitates, thereby lowering the purity of $Mg(OH)_2$ crystals precipitated from the brine.

In brine processing, the removal of boron is typically executed after the Mg^{2+} extraction step [4]. Several methods have been tested for B removal, such as chemical precipitation [12]; adsorption [10]; reverse osmosis; electrodialysis; solvent extraction and ion exchange [13]. Chemical precipitation is effective but requires adjusting the solution pH to high values (pH > 9), thus demanding large quantities of hydroxides [14] and resulting in co-precipitation with Mg, unless Mg has already been extracted. Other tested options rely on the addition of barium chloride to remove barium borate [7]. However, $BaCl_2$ is toxic and also hygroscopic. Adsorption of boron has been shown for MgO and CaO particles [10], but the use of this method is not adapted for brines, since the pH would change and a mixture of salts would be extracted, resulting in Mg loss. The use of electrodialysis and/or reverse osmosis would face scaling by divalent ions. Besides, this method has low selectivity when compared to the other cited methods. Extraction with solvents are considered highly selective for extraction of boron from complex salt lake brines [15–17]. However, they require low pH and the organic extractants are partially soluble in the brine. Thus, even though this method is currently in use for large volume brine processing [5], their use should be limited due to environmental risks.

Boron removal by a boron specific ion exchange resin was developed to remove borate from magnesium brine in the ceramic industry [18]. To our knowledge, only the extraction of boron from brines with lower concentrations of other ions, such as lithium and magnesium, has been considered so far [19–22]. The tested brine was already refined with only a residual Mg concentration of 0.6 ppm [19], i.e. several orders of magnitude lower than in Li^+ rich brines. Amberlite IRA743 was successfully used in the presence of Cl^- from sea water [23,24]. Moreover, the use of Amberlite does not require pH changes, as an almost constant uptake capacity is obtained between pH 4 and 9 [22]. The extraction of boron from native salt lake lithium rich brines thus warrants further investigation.

The present article has two principal aims: (i) to extract Mg^{2+} as chemical grade $Mg(OH)_2$ without Li^+ loss from the brine; (ii) to assess the selectivity of Amberlite IRA743 resin for boron extraction from salt lake brines containing Mg^{2+}. For that, the influence of different parameters (flow rate, temperature, pH and presence of other ions) on boron removal by the ion exchange resin was investigated in a column mode. Subsequently, the capacity of the native brine and the brine free of boron to precipitate $Mg(OH)_2$ was determined and the amount of Li^+ uptake in the solid, and purity of the precipitate were compared.

2. Materials and methods

2.1. Brine

Native brine from Salar de del Hombre Muerto (north-western Argentina) pumped by an Argentinean mining company was sampled for the experimental precipitation of $Mg(OH)_2$. The brine was analysed for major cation and boron compositions by inductively coupled plasma optical emission spectrometry (ICP-OES) and for major anions by ion chromatography (IC). The brine composition is shown in Table 1. Synthetic brine with the same composition was prepared for boron extraction optimization tests. LiCl (99%), NaCl (99.5%), KCl (99.5%), $MgCl_2{\cdot}6H_2O$ (99%), $CaCl_2{\cdot}2H_2O$ (99%), Na_2SO_4 (99%) and $Na_2B_4O_7{\cdot}10H_2O$ (99.5%) (all Sigma-Aldrich), and demineralized water were used.

The process used in this study to recover Mg^{2+} as $Mg(OH)_2$ compounds from the Salar de del Hombre Muerto brine included the following stages:

- Stage 1: B removal by Amberlite IRA743 (optimized on synthetic brine)
- Stage 2: Precipitation of $Mg(OH)_2$ by NaOH or CaO addition

Experiments shown in Figs. 1, 2, S2 and S3 were performed on synthetic brines (due to limited availability of natural brine). In turn, those experiments shown in figures S3, 3, 4, 5, 6, 7 and 8 were performed on real natural brine samples.

2.2. Boron removal by ion exchange resin

Amberlite IRA743 (Dupont) is based on a macroporous polystyrene matrix treated by chloromethylation and amination with N-methyl-D-glucamine. Boron can be retained according to the following reaction scheme: the borate ion is complexed by two sorbitol groups and a proton is retained by a tertiary amine site that behaves as a weakly basic anion exchanger (see Fig. S1(supplementary material)) [23]. The theoretical retention capacity reaches 5 to 7 mg/L but the practical capacity is inversely proportional to the flow rate due to mass transfer limitations [20].

A synthetic brine with chemical composition shown in Table 1 was used for optimization tests. The resulting pH of the synthetic brine was 7.8. Further pH modification were obtained with addition of NaOH or HCl. Column tests were performed in batch mode. The ion exchange columns, with inner diameter 2 cm, H = 50 cm, PTFE valve and a glass frit at the bottom, were filled in a volume of 100 ml (bed volume BV) with pre-weighted resin (76 g) generating a Height/diameter (H/D) ratio of 25. A syringe Pump (ProSense NE4000) was used to control the flowrate. Results are presented in breakthrough curves: a plot of the tested BV against the concentration of the adsorbate (boron and other ions) in the effluent stream.

The regeneration and reuse of the resins in multiple ion exchange cycles was examined. The following two regeneration methods were followed after the saturation of the resins.

Table 1
Composition of natural brines determined by ICP-OES analysis, used in this study. Cl^- and SO_4^{2-} determined by ion chromatography. Synthetic brine was also prepared to match this same natural brine composition.

Brine	Li^+	Ca^{2+}	Mg^{2+}	B	Na^+	K^+	Cl^-	SO_4^{2-}
mg/L	1,268	685	3,090	1,619	103,239	14,209	182,850	11,155

Method 1 - Hydroxide stabilization

- Regeneration was achieved using a 10 wt% H_2SO_4 solution (3 BV).
- Washing with 2.5 bed volumes of demineralized water.
- Stabilization of the resin by a 4 wt% NaOH solution (3 BV).
- Washing with 2.5 bed volumes of demineralized water.

Method 2 - Hydroxide partial stabilization

- Regeneration was achieved using a 10 wt% H_2SO_4 solution (3 BV).
- Washing with 2.5 bed volumes of demineralized water.
- Stabilization of the resin by a 4 wt% NaOH solution (1 BV).
- Washing with 5 bed volumes of demineralized water.

Chemical and physical properties of the resin are presented in Table S1(supplementary material).

2.3. $Mg(OH)_2$ Precipitation

Experimental tests were performed in triplicate to remove magnesium from native Li^+ rich brines. For each test, 50 ml of brine was added to 60 ml falcon tubes (reactors). The precipitating reagent (NaOH or CaO) was added to the reactor in solid form in each experiment. The effect of the different chemicals and amount added (0.50 g and 0.56 g) of NaOH and (0.70 g and 0.78 g) for CaO (1.0 or 1.1 times the stoichiometric amount to form $Mg(OH)_2$) was examined.

The brine and the reactants were mixed at a stirring rate of 350 rpm using a magnetic stirrer, (magnetic stirrer bar of 1 cm was added inside of the falcon tubes, and the falcon tubes were placed upside-down in the magnetic plate) at a temperature of 20 °C for 2 h. After continuous stirring (2 h), samples were positioned for the sedimentation test (72 h). Subsequently, the precipitates were centrifuged at 14560 × g for 10 min, retaining the solid precipitate and obtaining the low Mg^{2+} concentration brine. The precipitates were washed with de-ionized water (single wash with 10 ml water for a cake formed from 50 ml of treated brine). The solids were dried in an oven at 105 °C for 48 h. Finally, the dry solid was ground into a uniform powder with a ceramic mortar and pestle, for further analysis.

2.4. Analytical methods

Metal concentrations were determined using inductively coupled plasma optical emission spectrometry (ICP-OES, Thermo Scientific iCAP 7400), after dilution with 1 (v/v) % HNO_3 (Chem-Lab, Belgium). Quantification was performed using external standards in the 0 – 20 mg L^{-1} concentration range and guaranteed by analyzing a quality control standard after each series of 30 samples. Ion chromatography (IC) (ICS-2000, Dionex) was used after dilution with demineralized water. X-ray diffraction (XRD) measurements were carried out on a Bruker D8 Discover XRD system equipped with a Cu X-ray source ($\lambda = 1.5406$ Å) and a linear X-ray detector. The samples were put on a Si sample cup on the sample stage. $\theta - 2\theta$ measurements were carried out in air at atmospheric pressure, step size was 0.05° and count time per step was 2 s. TEM images, selected-area electron diffraction patterns (SAED) and energy dispersive X-ray (EDX) analyses of precipitates were collected on a JEOL JEM-2200FS FEG Transmission Electron Microscope (TEM) (200 kV). In the SAED patterns, reciprocal lattice distances were directly measured using *Image J* software with *CalcdSpace* plugin.

3. Results and discussion

3.1. Effects of brine flow rate, pH, temperature and other ions on boron removal

The effects of parameters such as brine flow rate, temperature, pH and the presence of other anions on boron intake by Amberlite IRA743 were investigated in the literature [19]. However, all previous works involved lower salinity aqueous solutions, with concentrations of B below 100 ppm (1619 ppm here, see table 1). The column mode operation was used to investigate the parameters' influence on the boron extraction from synthetic Li^+ rich brine, boron concentration of 1.6 g L^{-1}, and H/D ratio of 25 were kept constant for all the experiments.

The effect of brine flow rate on boron removal was examined at 0.1, 0.5, 1 and 3 BV/h. The temperature was 20 °C and solution pH was 7.8. The breakthrough curves of boron for different flow rates are given in Fig. 1.

As shown in Fig. 1, the faster the flow rate, the sooner the breakthrough. This phenomenon was observed before [22,24], and can be explained as follows: as the flow rate of brine increases, the contact time between resin and brine is shortened. Therefore, there is not enough time for the resin to adsorb all the boron at the high brine flow rate, and the breakthrough point is reached sooner with low boron removal. The results showed that the time to reach the breakthrough point is short due to the initial high boron concentration, and consequent fast saturation of sorption capacity of the resin.

The capacity of boron uptake by the resin was 1.60, 2.48, 3.25 and 4.57 g_B L^{-1} for 3; 1; 0.5 and 0.1 BV/h volumetric flow rate respectively. When compared with the literature, the capacity of boron uptake by Amberlite IRA 743 is superior in this work than previously reported. Simonnot et al. [25] obtained a boron uptake by the resin of 2.3 g_B L^{-1} for solutions with boron concentration between 20 and 100 mg L^{-1} (flow rate 1.2BV/h). The same work also showed that an increase in the initial boron concentration in solution increased the boron uptake of resin, which is in line with results reported here. The uptake of boron increases with the initial concentration because Amberlite resins work

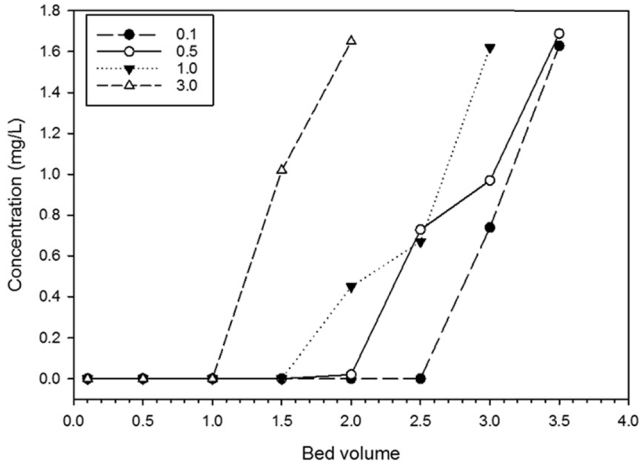

Fig. 1. Breakthrough curves, boron concentration (g L^{-1}) in the effluent after column tests using Amberlite IRA743 with initial boron concentration of 1.6 g L^{-1} and different flow rates of 0.1, 0.5 and 3 BV/h (results were obtained with synthetic brine).

by complexation and not by a reversible adsorption process [18].

The effect of temperature on boron removal was examined at 20, 40, and 60 °C, with brine flow rate of 0.1 BV/h, and pH at 7.8. The results (Fig. S2 (supplementary material)) showed that in terms of uptake capacity, the effect of temperature is not significant in the range 20 – 60 °C. There is a contradiction in the literature about temperature influence, some works have found that the boron removal rate increased with increasing temperature, while others reported no effect [19,22]. The explanation was that as the temperature rises, the Brownian motion of boron is accelerated, and such acceleration facilitates the diffusion to the resin surface and the complexation process. However, when the contact time is long enough to promote all the possible complexation, i.e. when the flow rate is low enough to not make diffusive flux limiting, the temperature has no significant influence. Since our experiments were carried out at long contact time, it is reasonable to expect that temperature does not affect the uptake capacity. This is good news in the perspective of industrial applications, since heating of huge volumes of brines, would considerably increase the cost of brine processing.

The effect of pH on boron removal was examined at pH 7, 8, and 9, with brine flow rate of 0.1 BV/h, and temperature at 20 °C. Further changes in pH are beyond the scope of this work. Larger pH changes would signify higher addition of chemicals to brines, while pH higher than 9 should be avoided to circumvent $Mg(OH)_2$ precipitation. The boron uptake values for the resin ($g_B\,L^{-1}$) obtained at different pH values are plotted in Fig. 2. Boron complexation increases with pH in the range of 7 to 9. The pH dependence of boron uptake is related to the speciation of B in aqueous solutions: at lower pH, $B(OH)_3$ predominates, and with increasing pH more boron is present as $B(OH)_4^-$. The latter forms a bidentate complex with two N-methyl-D-glucamine groups of the resin [26], see Fig. S1 (supplementary material). Previously, it has been shown that the resin's hydroxyl groups have higher affinity for $B(OH)_4^-$ ions, as compared with $B(OH)_3$ species, and that in case of a pH lower than 7 the selectivity for B removal decreases [26,27]. The pH of the natural brine was determined to be 7.8. In this case, in the perspective of industrial application, a careful balance between the convenience of changing the pH to large brine volumes, to increase the removal capacity per unit mass of resin should be analyzed.

Since the behavior of natural brines has sometimes been reported to differ from that of simulated brines, boron removal from a natural Li^+ rich brines with Amberlite IRA743 resin was explored for the following results. A natural brine flow rate of 0.1 BV/h was used, temperature at 20 °C, and the pH 7.8 of the natural brine was not changed. The breakthrough curve (Fig. S3 (supplementary material)) obtained is similar to the curve presented in Fig. 1., essentially showing no changes between experiments on simulated and natural brine on boron removal.

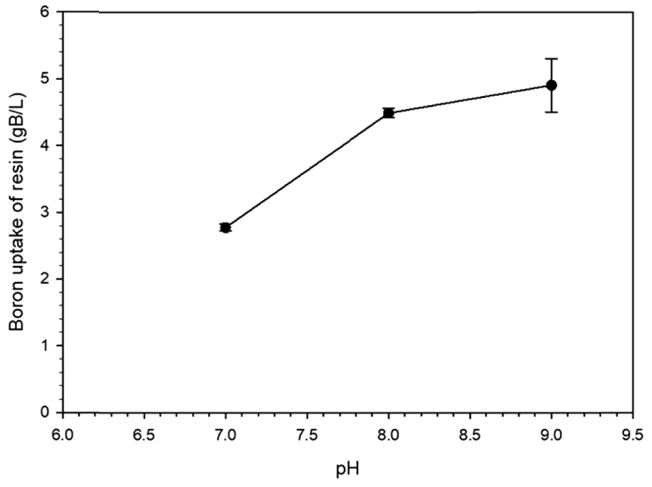

Fig. 2. Boron uptake by Amberlite IRA743 resin for different pH values (results were obtained with synthetic brine).

These data prove that the capacity of boron complexation by Amberlite is not lost in natural Li^+ rich brines. Similar results have been published before for lower concentrations of salts [19,24,25].

While there was no apparent effect of other ions on the boron uptake capacity, it is also important to verify the Li^+ concentration, before and after Amberlite treatment. Complexation of Cl^- by the resin is expected to occur only when the $B(OH)_4^-$ concentration is scarce. Cations loss to the resin was not expected as the resin is designed to complex anions. Fig. 3 a. shows Na^+, Li^+, Mg^{2+} and Cl^- concentration in the brine after treatment with ion exchange resins for different BV. The loss of Cl^-, Li^+ and Mg^{2+} was observed during the first 2 bed volumes (the first 200 ml of treated brine) and had a constant decrease with the treatment. After 2BV the concentration of Li^+, Mg^{2+} and Cl^- in the treated brine was the same as in the raw brine. This observation showed that the uptake of other ions was related to the beginning of treatment or resin regeneration process performed prior to the polishing experiment.

The regeneration process consists of two main steps, boron removal from the resin using acid regenerants, followed by neutralization of the resin with alkali solutions. Kalaitzidou et al. [22] studied the influence of different regeneration processes for Amberlite, and observed that, after stabilization of the resin using NaOH (pH 12.5), several bed volumes presented high pH values.

The loss of Mg observed in the current work (Fig. 3 a) can therefore be explained by the formation of some $Mg(OH)_2$ in the first bed volumes of the column when the pH is still high. In turn, Li^+ is most likely lost trapped in the $Mg(OH)_2$ precipitate, as explained above. Stabilization with $NaHCO_3$ was able to keep the pH constant at 8.5 [22]. However, this is not an option for the current work, as the presence of HCO_3^- would cause the precipitation of $CaCO_3$ inside of the column upon brine flooding. We have tested different approaches for regeneration/stabilization and determined that the best option to avoid Mg^{2+} and Li^+ lost was the use of a 4% NaOH solution, with a flowrate of 1 (BV/h) and a total volume of 1 BV followed by water rinsing at a flowrate of 1 BV/h, for a total volume of 5 BV. In that case, we have a low addition of NaOH and part of the resin maintains the complex with SO_4^{2-} from the acid regeneration. This modified stabilization process resulted both in brine chemical characteristics conservation, i.e. a minimal loss of cations in the first two BV (Fig. 3 b), while no changes in B uptake were observed (Fig. 3 b). In the remainder of this work, the resin was regenerated using Method 2.

To evaluate the effect of multiple regeneration cycles, boron removal from natural Li^+ rich brines with Amberlite IRA743 (3.5 BV) followed by Method 2 regeneration resin was explored for 10 cycles. The brine flow rate of 0.1 BV/h, the temperature at 20 °C, pH 7.8 were kept constant. Boron uptake for the 10 different cycles was the same, with 4.57 $g_B\,L^{-1}$ for the first cycle and 4.62 $g_B\,L^{-1}$ for the tenth cycle showing outstanding regeneration characteristics of the resin. Li^+ concentration was also checked for a brine treated with a 10 times regenerated resin and showed no Li loss.

3.2. Effect of B removal on Mg recovery

In the following section, the effects of B removal on solid precipitation, $Mg(OH)_2$ purity and Li^+ loss is investigated.

3.2.1. Influence of the nature and concentration of the base precipitant

The effect of different bases (NaOH and CaO) and amount added (1.0 or 1.1 times the stoichiometric concentration related to $Mg(OH)_2$) was examined for samples that had, or had not been treated previously with Amberlite IRA743 (i.e., B had or had not been previously removed). Fig. 4. shows the decrease in sedimentation height for 8 different experiments during 2 h upon base addition. The initial sediment height was always 100 mm, which implies that the crystals are dispersed in the entire solution with no sedimentation. For the subsequent period the presented height represents the cake volume, which is formed by the amount of solid precipitated plus the volume of occluded brine. The

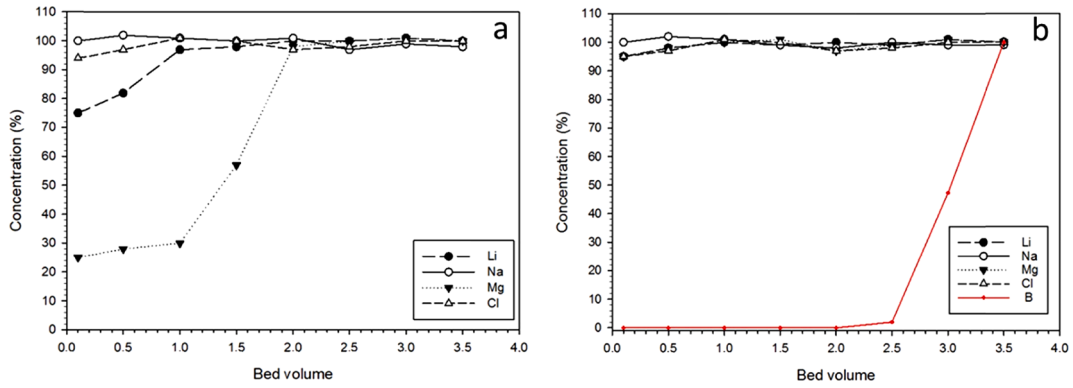

Fig. 3. Na^+, Li^+, Mg^{2+} and Cl^- concentration variations during boron extraction process with Amberlite IRA743: (a) Method 1 - Hydroxide stabilization; (b) Method 2 – Partial hydroxide stabilization.

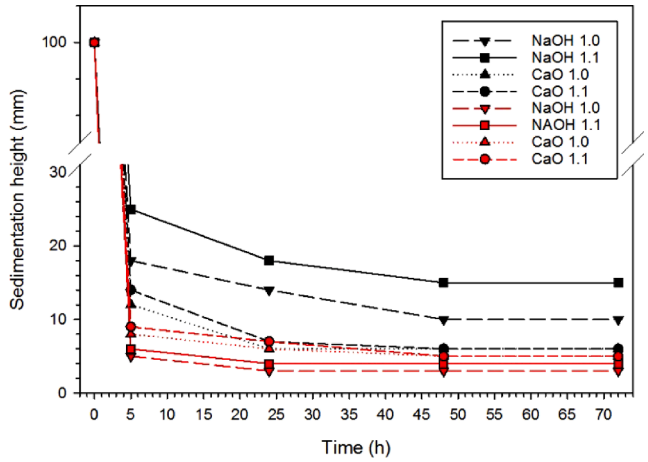

Fig. 4. Sedimentation height variation with time for brines with B (black) and without B (red). The figure caption indicates the nature and the stoichiometric amount, relative to $Mg(OH)_2$, of the base used.

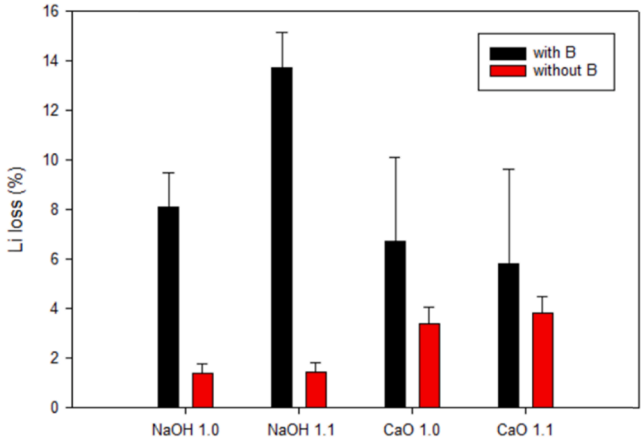

Fig. 5. Li^+ loss during $Mg(OH)_2$ crystallization from brines with and without B, for different bases.

addition of CaO, traditionally used for Mg^{2+} removal in the current technology for Li_2CO_3 production, showed faster sedimentation and smaller final cake. Besides, the results for CaO induced precipitation with or without B are similar, i.e. the presence of B shows little influence on crystals sedimentation. In contrast, precipitation induced by NaOH shows a strong influence of the B presence. Samples free of B have faster sedimentation and smaller final cake volume. Additionally, the amount of base added for the crystallization has little influence for samples free of B; however, the addition of 10% more NaOH to natural brine increased the volume of the final sediment by 52%, probably related to other salts precipitated composed by Ca^{2+} and B. It is worth noting that, in the absence of B, NaOH additions lead to slightly smaller final cake volumes, than for CaO additions.

Larger cake volumes due to brine trapping within the cake result in decreased filterability of the suspensions and in increased Li^+ loss. Li^+ loss was calculated based on the mass of brine trapped in the cake after centrifugation, by the subtraction of the dry cake weight from the weight before the drying process (48 h at 105 °C), considering the brine density value of 1.26 g/cm^3, to estimate the volume of trapped brine, and the raw brine Li^+ original concentration.

Samples with B present resulted in higher final cake volume, showing higher Li^+ loss for all the applied conditions (Fig. 5.). A Li^+ loss of 13.7 ± 1.2% is observed when 1.1 stochiometric amount of NaOH is added and 8.1 ± 1.0% in the presence of 1.0 stoichiometric amount of NaOH. The extraction of B before precipitation produces a sharp decrease in these numbers to 1.5 ± 0.4 and 1.4 ± 0.4%, respectively. As it was already mentioned, the B presence has less influence when CaO is used as the base form to induce precipitation. Lower Li^+ loss is also observed in the CaO method when B is absent from the brine. However, the lowest Li^+ loss is observed upon B extraction prior to addition of NaOH when compared with the traditional alkalizing agent CaO. In other words, the optimal $Mg(OH)_2$ crystallization, from the perspective of achieving the lowest amount of Li^+ loss, is via B removal followed, by NaOH addition.

In addition to the Li^+ loss, the cake size will naturally correlate with

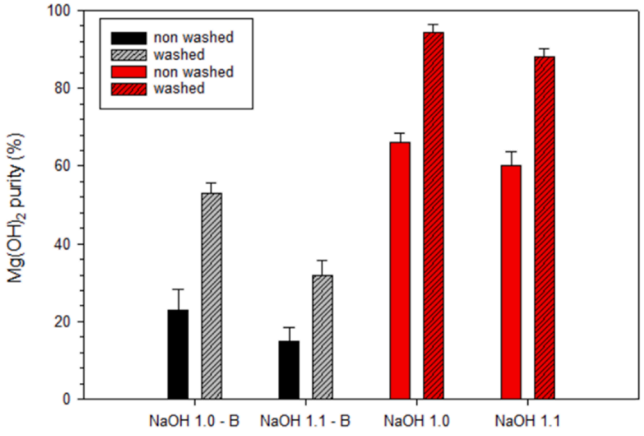

Fig. 6. $Mg(OH)_2$ purity before and after washing. Solid samples precipitated upon addition of NaOH to brines with (black) and without (red) B. 10 ml demineralized water was used to wash the solid generated from 50 ml of brine.

the $Mg(OH)_2$ purity, since the trapped brine occludes 317 g other salts per liter. Fig. 6. shows the purity of $Mg(OH)_2$ for samples where NaOH was used as the alkalizing agent. Results on samples precipitated with the addition of CaO are not presented here as the precipitates obtained are a mixture of $Mg(OH)_2$ and $CaSO_4$ (Fig. 7.a). With the aim of avoiding extra water usage in the Li extraction from brines, sample purity was initially measured for samples without a washing step. Subsequently, a washing step with a low water volume (Fig. 6) was conducted to investigate the impact of washing on $Mg(OH)_2$ purity. The water used for washing could potentially be added to the treated brine to increase Li^+ recovery, although this would imply a dilution of the natural brine, which ideally should be avoided. We can also envision that the washing of the solid could be performed in an alternative location, where water is a much more abundant resource than in the arid lands in the vicinity of lithium mining facilities. It is very unlikely that Mg(OH)2 will be used in the vicinity of the said mining facility, i.e. transport of the product is needed in any case. $Mg(OH)_2$ purity directly precipitated from natural brine is inferior to 25%; the washing process improves the purity to 53% (Fig. 6). The B extraction pretreatment increases the $Mg(OH)_2$ purity to over 60% before washing, and the washing process yields $Mg(OH)_2$ with 95% purity. The main compound that is removed by the washing step is NaCl (Fig. 7b), which is to be expected, since this was the most concentrated salt in the natural brine.

3.2.2. *Characterization of solid precipitates*

Brucite ($Mg(OH)_2$) was observed using XRD in samples prepared in the absence (Fig. 7a and b) and presence (Fig. 7c) of boron. However, when CaO was used as base precipitant, bassanite ($CaSO_4$* ½ H_2O) was also detected. In addition, when NaOH was added as base, some NaCl was observed. In all cases, the peaks observed for brucite show a broad full-width at half maximum (FWHM, see also Figure S4 (supplementary material)) compared to the crystalline standard pattern, suggesting that the brucite is either very fine-grained, the crystal structure shows some disorder, or both.

Brucite has a layered crystal structure [28,29] and these layers are held together weakly by van der Waals forces [30], although some experimental results suggest a degree of hydrogen bonding [31,32]. Brucite and other divalent metal hydroxides with similarly layered crystal structures are known to adsorb large amounts of water and oxyanions including borate ($B(OH)_4^-$) in their interlayers, forming layered double hydroxides [33]. The interlayer distance for the (0 0 1) *d*-spacing observed in XRD patterns, depends, among other factors, on the size and charge of oxyanions present in the interlayer [33]. Moreover, many other divalent metal ions can adsorb as well, or substitute for magnesium into the crystal structure [34], altering the adsorption capacity of the precipitate for anions while also potentially shifting the peaks in the XRD patterns.

The peak around $2\theta = 18.6°$ represents the (0 0 1) basal plane *d*-spacing for brucite, which has a distance of 4.77 Å between the layers in the crystal structure. In the presence of boron, this plane is strongly affected, showing a doublet peak (Fig. 7c, d), rather than the single peak observed for the B-free experiments (Fig. 7b). The maxima of this doublet lie around $2\theta = 18.0°$ (4.94 Å) and $2\theta = 19.3°$ (4.6 Å). The first of these peaks coincides with the (−1 1 1) d-spacing of hydroboracite (4.95 Å), although no other hydroboracite d-spacings were observed (Figure S4 (supplementary material)). The second maximum of the doublet, at $2\theta = 19.3°$, is not directly related to a d-spacing of brucite or hydroboracite. It might be related to the (0 0 1) for brucite, shifted to higher 2θ values and therefore to smaller d-spacing, although it is unclear what would cause a decrease in brucite interlayer distance. Alternatively, this peak might be caused by convolution of the (0 0 1) d-spacing of brucite and the (1 1 1) d-spacing of hydroboracite (at $2\theta = 19.9°$). Also note that the brucite (1 0 0) and (1 1 0) remain fairly unaffected in the presence of boron (Figure S4 (supplementary material)). This may be supportive of a local impact of boron uptake on the brucite structure that only affects d-spacings related to the interlayer distance,

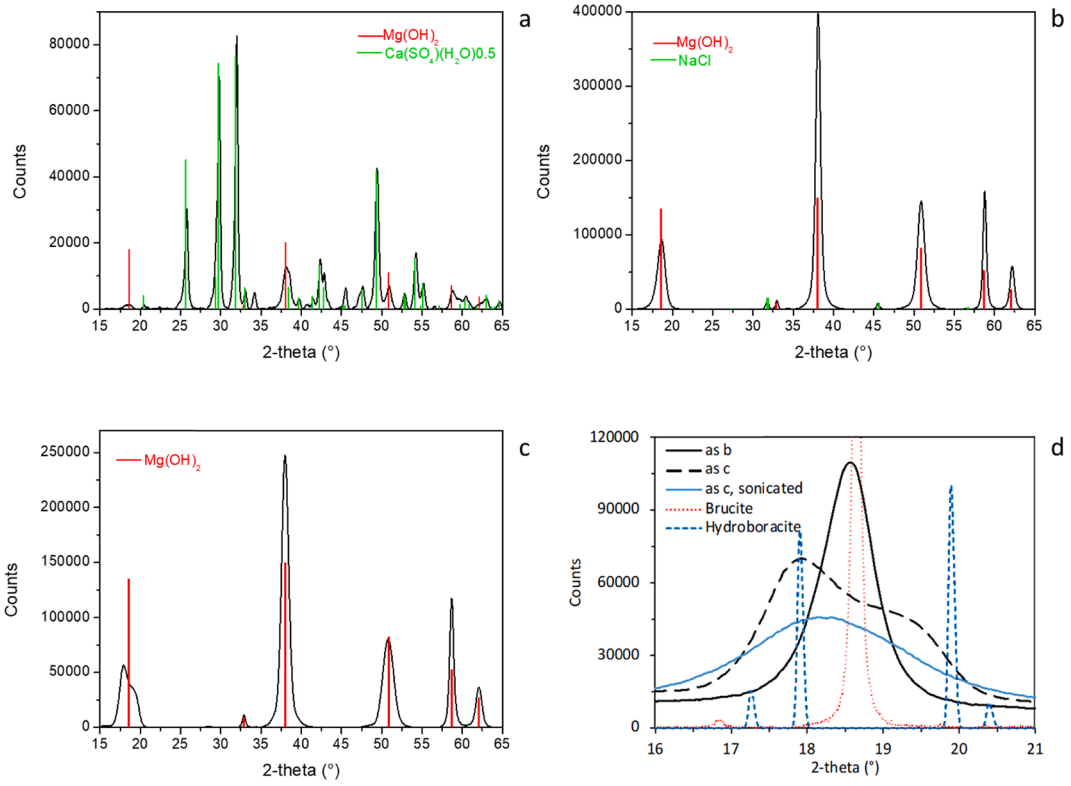

Fig. 7. XRD patterns for various solid samples (washed samples) crystallized upon base addition to brines. Solids formed upon addition of a) 1.1 CaOH to B-free brine; b) 1.1 NaOH to B-free brine; c) 1.1 NaOH to B-containing brine. d) zoom on 2θ values of 16-21° for patterns shown in b (solid black line) and c (long-dashed black line), (solid blue line) samples prepared in the presence of boron under ultrasound.

such as the (0 0 1), while the (1 0 0) and (1 1 0) remain unaffected. To summarize, the XRD patterns show that the presence of B affects the interlayer distance of brucite, suggesting borate co-precipitation or hydroboracite intercalation occurs when $Mg(OH)_2$ precipitates from the B-containing brine. So, it is quite likely that the hydroboracite is present as a local structure on the (0 0 1) basal plane of brucite. In this case, hydroboracite is placed between two brucite layer in a sandwich structure. This distortion on brucite structure increases the structure total brine entrapment and can explain the result showed in Fig. 4.

Thermodynamic calculations using PHREEQC (SI Table S2 (supplementary material)) indicate that the brine itself is indeed highly supersaturated with respect hydroboracite and remains supersaturated upon base additions up to pH > 10.5. Note also that the brine is initially undersaturated with respect to brucite and only becomes supersaturated when the solution reaches pH ≥ 9.5, due to base addition. So, it is likely that hydroboracite forms initially, and when pH increases beyond 10.5 it would start re-dissolving. However, since brucite is also precipitating, some of the hydroboracite might become occluded in brucite. Potentially, brucite protects the hydroboracite from dissolving, explaining the observed hydroboracite *d*-spacing in the XRD pattern. However, based on XRD and PHREEQC calculations alone it cannot be determined if this is as a separate phase or a solid-solution/intercalation with brucite.

In order to determine whether the hydroboracite is present as intercalation within the brucite or as a separate compound, additional samples were precipitated under ultrasound (ultrasound bath at 35 kHz). It was expected that, if the hydroboracite was present as an intercalation, this structure would be disrupted more easily by the ultrasound, potentially resulting in a loss of the hydroboracite *d*-spacings while only specific *d*-spacings for brucite would be affected. Contrastingly, if a mixture of independent grains was present, these grains were expected to be affected similarly. Brucite has a slightly harder crystal structure (Mohs scale hardness 2.5–3) than hydroboracite (Mohs scale 2), although brucite fractures easily and perfectly along its basal (0 0 1) plane.

Crystallization under ultrasound yielded smaller sediment volume (9 mm sedimentation height for additions of 1.1 NaOH instead of 18 mm) with a less gelatinous character, lower amounts of trapped brine and a drop in the Li^+ loss from 13 to 6%. Given that borate is known to form gel like substances, these observations could be due to the ultrasound breaking a borate (hydro-)gel [35], or hydroboracite intercalations that potentially hold more brine. Ultrasound can also be responsible for a higher brucite crystallinity.

The small-angle XRD pattern for the precipitate formed in ultrasound is shown as a solid blue line in Fig. 7d, and the full pattern is shown in Fig. S4 (supplementary material). It shows that the doublet peak is indeed disrupted into a single broad peak at a *d*-spacing approximately half-way between the (0 0 1) for brucite and the (−1 1 1) for hydroboracite. The other d-spacings all show slightly broader FWHM, more strongly so for the (0 1 2) and (1 0 3) than the other *d*-spacings. This indicates that the brucite has decreased long range ordering in particular along the c-axis, either by fracturing along the (0 0 1) cleavage planes, or by breaking the hydroboracite intercalation.

The TEM analysis and the electron diffraction patterns, Selected Area Electron Diffraction (SAED), for samples prepared in the absence of

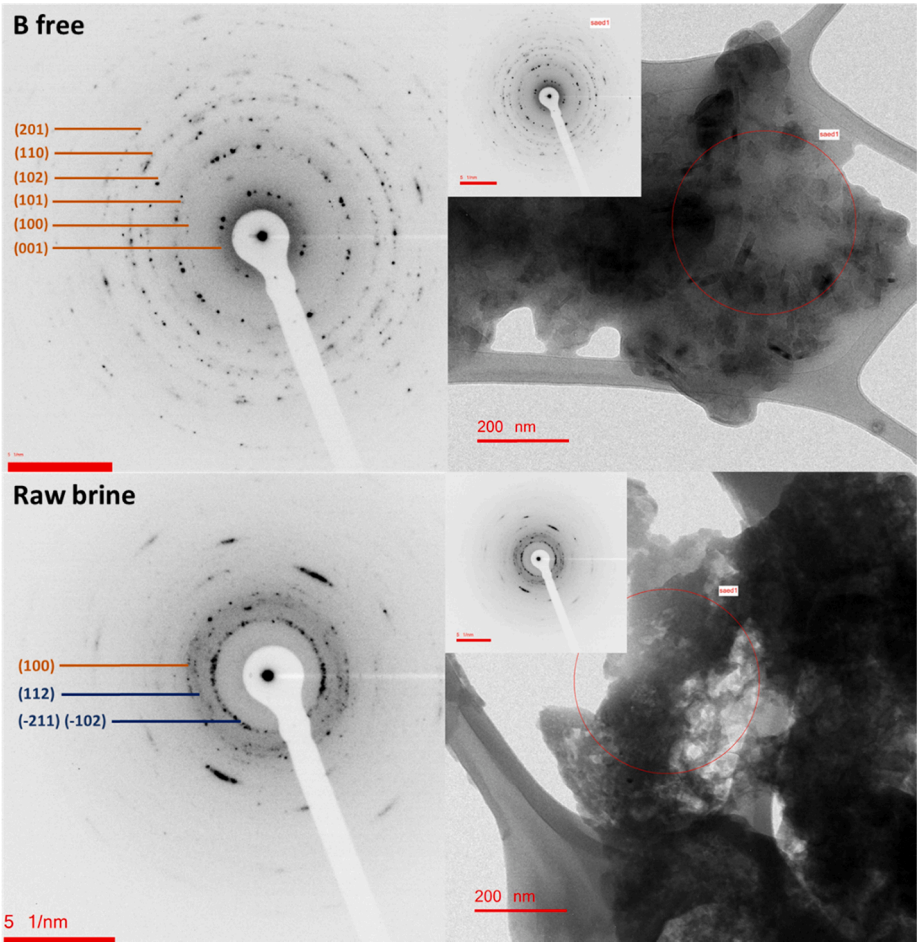

Fig. 8. TEM images of $Mg(OH)_2$ particles prepared by precipitation method with NaOH addition. The left images show SAED pattern of the samples. Top images are from a sample free of B, and bottom images are from natural brine. hkl corresponding to brucite are presented in orange and possible correspondence to hydroboracite are presented in blue.

boron present a typical result for $Mg(OH)_2$ (Fig. 8). The pattern revealed a textured ring due to the polycrystalline character of the brucite phase, with a certain degree of disorder. All *d*-spacing from (001) to (201) (Table S3 (supplementary material)) can be measured, confirming the crystalline structure of the particles. The crystals are presented in a massive aggregate with many crystals visible that have a rode/needle-like structure. The tendency of brucite to form a nest-like aggregation of thin nanosheets was described before [36]. Crystals are generally smaller than 100 nm, supporting the fine-grained nature, leading to broad FWHM in the XRD patterns. The SAED pattern also confirms this, with various crystals contributing to the pattern, leading to rings with different, more intense diffraction spots.

Samples prepared from natural brine present some degree of crystallinity from the SAED patterns, but less than in samples free of B (Fig. 8), the patterns revealed a high textured ring with some intersection between different rings due to the polycrystalline character of the brucite phase, and the presence of hydroboracite inducing a certain degree of disorder. The measurement of the d-spacing from SAED pattern reveals the (100) *d*-spacing from brucite and a possible presence of (112), (−211) and (−102) from hydroboracite. The crystals observed are finely grained with particles of approximately 20 nm in size. There is again an aggregate, but this appears less massive. No larger and clearly distinguishable crystals are present, and this is also the case for samples free of B.

4. Conclusions

Traditionally, alkalizing agents, such as lime, have been employed to raise the pH levels of Li^+ rich brines and induce Mg precipitation as $Mg(OH)_2$. The addition of lime produces the precipitation of a mixture of $Mg(OH)_2$ and $CaSO_4$. The combination of these mixed crystals blocks the recovery of Mg products and creates a considerable volume of waste during Li_2CO_3 extraction. The addition of NaOH as alkalizing agent enables the precipitation of $Mg(OH)_2$ unaccompanied by other salts. However, the B presence in the brine increases the volume of the sediment and traps close to 15% of the brine in the cake, generating high Li^+ loss and low purity of $Mg(OH)_2$ crystals. Here we have shown that the extraction of B prior to $Mg(OH)_2$ precipitation enables the crystallization of $Mg(OH)_2$ crystals with 95% purity. This research is relevant both in the perspective of brine alkalinization via addition of chemicals, as performed here, and also in light of electrochemical generation of OH^- via water reduction [7].

The present article had 2 principal aims: (i) the extraction of Mg as chemical-grade $Mg(OH)_2$ without Li^+ loss and (ii) to assess Amberlite IRA743 resin selectivity for boron extraction from extreme salinity brines with high Mg^{2+} concentration.

- It was possible to selectively extract B from salt lake brines with minimal loss of Mg^{2+} or Li^+
- It was shown that resin saturated with boron could be efficiently regenerated and reused after treatment with H_2SO_4 solutions followed by NaOH reconditioning.
- It was shown that precipitation with CaO as an alkalizing agent generates a mixture of crystals and a Li^+ loss of between 7 and 4%.
- It was possible to reduce Li^+ loss to values as low as 1.4% during $Mg(OH)_2$ precipitation from brines free of B.
- Chemical-grade $Mg(OH)_2$ precipitation was possible from brines free of B.
- The high water intake shown in the presence of B was associated with the presence of hydroboracite in intercalation within the brucite crystal.

Finally, the use of NaOH to replace CaO represents an increase in cost in the first moment. However, this change enables the recovery of a Critical metal, Mg as $Mg(OH)_2$, that can be sold and avoid waste discharge.

Declaration of Competing Interest

The authors declare that they have no known competing financial interests or personal relationships that could have appeared to influence the work reported in this paper.

Acknowledgement

The authors wish to acknowledge financial support from the ERA-MIN2 research project entitled “Membrane electrolysis for resource-efficient lithium and water recovery from brines” (Acronym: Li + WATER). LB is supported by the Fonds voor Wetenschappelijk Onderzoek - Vlaanderen (FWO) PROJECT 3G0I1818W. KR is supported by a Ghent University Bijzonder Onderzoeksfonds GOA grant (BOF19/GOA/026). VF is a permanent research fellow from CONICET. This project has received funding from the European Research Council (ERC) under the European Union’s Horizon 2020 research and innovation programme (grant agreement No. 819588) to M. Wolthers. Minera Santa Rita (Argentina) is gratefully acknowledged for providing the Li + rich brine.

Appendix A. Supplementary material

Supplementary data to this article can be found online at https://doi.org/10.1016/j.seppur.2021.119177.

References

[1] L. Talens Peiró, G. Villalba Méndez, R.U. Ayres, Lithium: Sources, production, uses, and recovery outlook, Jom. 65 (2013) 986–996, https://doi.org/10.1007/s11837-013-0666-4.
[2] Y. Pranolo, Z. Zhu, C.Y. Cheng, Separation of lithium from sodium in chloride solutions using SSX systems with LIX 54 and Cyanex 923, Hydrometallurgy. 154 (2015) 33–39, https://doi.org/10.1016/j.hydromet.2015.01.009.
[3] V. Flexer, C.F. Baspineiro, C.I. Galli, Lithium recovery from brines: A vital raw material for green energies with a potential environmental impact in its mining and processing, Sci. Total Environ. 639 (2018) 1188–1204, https://doi.org/10.1016/j.scitotenv.2018.05.223.
[4] D. Garrett, Handbook of Lithium and Natural Calcium Chloride., Elsevier, Science. (2004).
[5] D.E. Garrett, Handbook of Lithium and Natural Calcium Chloride, Elsevier, 2004.
[6] Y. Zhang, Y. Hu, L. Wang, W. Sun, Systematic review of lithium extraction from salt-lake brines via precipitation approaches, Miner. Eng. 139 (2019), 105868, https://doi.org/10.1016/j.mineng.2019.105868.
[7] C.H. Díaz Nieto, N.A. Palacios, K. Verbeeck, A. Prévoteau, K. Rabaey, V. Flexer, Membrane electrolysis for the removal of Mg2+ and Ca2+ from lithium rich brines, Water Res. 154 (2019) 117–124, https://doi.org/10.1016/j.watres.2019.01.050.
[8] A.N. Løvik, C. Hagelüken, P. Wäger, Improving supply security of critical metals: Current developments and research in the EU, Sustain. Mater. Technol. 15 (2018) 9–18, https://doi.org/10.1016/j.susmat.2018.01.003.
[9] European Commission, On the review of the list of critical raw materials for the EU and the implementation of the Raw Materials Initiative, 2014.
[10] M. Del Mar De La Fuente Garcia-Soto, E.M. Camacho, Boron removal by means of adsorption with magnesium oxide, Sep. Purif. Technol. 48 (2006) 36–44, https://doi.org/10.1016/j.seppur.2005.07.023.
[11] S. Izawa, C. Tokoro, K. Sasaki, F. Futami, Clarification for removal mechanism of Boron using co-precipitation with magnesium hydroxide, (n.d.) 46–51.
[12] D.E.P. Pct, P. Ct, Wo 2013/049952, (2013).
[13] D.E. Garrett, Borates- Handbook of Deposits, Properties, and Use, Academic Press, Processing, 1998.
[14] D. A.Boryta, Removal of boron from lithium chloride brine, 1981.
[15] J.R. Kumar, C.J. Kim, H.S. Yoon, D.J. Kang, J.Y. Lee, Recovery of boron and separation of lithium from uyuni salar brine using 2,2, 4-trimethyl-1,3-pentanediol (TPD), J. Korean Inst. Met. Mater. 53 (2015) 578–583, https://doi.org/10.3365/KJMM.2015.53.8.578.
[16] R. Zhang, Y. Xie, J. Song, L. Xing, D. Kong, X. Li, T. He, Hydrometallurgy Extraction of boron from salt lake brine using 2-ethylhexanol, Hydrometallurgy. 160 (2016) 129–136, https://doi.org/10.1016/j.hydromet.2016.01.001.
[17] J.W. An, D.J. Kang, K.T. Tran, M.J. Kim, T. Lim, T. Tran, Recovery of lithium from Uyuni salar brine, Hydrometallurgy. 117–118 (2012) 64–70, https://doi.org/10.1016/j.hydromet.2012.02.008.
[18] N. Hilal, G.J. Kim, C. Somer, Boron removal from saline water : A comprehensive review 273 (2011) 23–35, https://doi.org/10.1016/j.desal.2010.05.012.
[19] C. Yan, W. Yi, P. Ma, X. Deng, F. Li, Removal of boron from refined brine by using selective ion exchange resins, J. Hazard. Mater. 154 (2008) 564–571, https://doi.org/10.1016/j.jhazmat.2007.10.067.
[20] C. Jacob, Seawater desalination : Boron removal by ion exchange technology 205 (2007) 47–52, https://doi.org/10.1016/j.desal.2006.06.007.

[21] M. Parsaei, M.S. Goodarzi, Adsorption Study for Removal of Boron Using Ion Exchange Resin in Bach, System 6 (2011) 398–402.
[22] K. Kalaitzidou, A.M. Tzika, K. Simeonidis, M. Mitrakas, Evaluation of boron uptake by anion exchange resins in tap and geothermal water matrix, Mater. Today Proc. 5 (2018) 27599–27606, https://doi.org/10.1016/j.matpr.2018.09.080.
[23] A. Alharati, J. Valour, S. Urbaniak, Y. Swesi, K. Fiaty, C. Charcosset, Chemical Engineering & Processing : Process Intensi fi cation Boron removal from seawater using a hybrid sorption / micro fi ltration process without continuous addition of resin 131 (2018) 227–233, https://doi.org/10.1016/j.cep.2018.07.019.
[24] N. Bin Darwish, V. Kochkodan, N. Hilal, Boron removal from water with fractionized Amberlite IRA743 resin, Desalination. 370 (2015) 1–6, https://doi.org/10.1016/j.desal.2015.05.009.
[25] M. Simonnot, C. Castel, M. Nicolaiè, C. Rosin, M. Sardin, H. Jauffret, Â. Chimique-cnrs-ensic, Â.E. De Volvic, V. Cedex, G. Pe, BORON REMOVAL FROM DRINKING WATER WITH A BORON SELECTIVE RESIN : IS THE TREATMENT REALLY SELECTIVE ?, 34 (2000) 109–116.
[26] M.A. Kamboh, M. Yilmaz, Synthesis of N -methylglucamine functionalized calix [4] arene based magnetic sporopollenin for the removal of boron from aqueous environment, DES. 310 (2013) 67–74, https://doi.org/10.1016/j.desal.2012.10.034.
[27] X. Li, R. Liu, S. Wu, J. Liu, S. Cai, D. Chen, Journal of Colloid and Interface Science Efficient removal of boron acid by N-methyl- D -glucamine functionalized silica – polyallylamine composites and its adsorption mechanism, J. Colloid Interface Sci. 361 (2011) 232–237, https://doi.org/10.1016/j.jcis.2011.05.036.
[28] M. Catti, G. Ferraris, S. Hull, A. Pavese, Static compression and H disorder in brucite, Mg(OH)2, to 11 GPa: a powder neutron diffraction study, Phys. Chem. Miner. 22 (1995) 200–206, https://doi.org/10.1007/BF00202300.
[29] F. Zigan, R. Rothbauer, N. Jahrb, Fuer Miner, Monatshefte. 4 (1967) 137.
[30] P. D'Arco, M. Causà, C. Roetti, B. Silvi, Periodic Hartree-Fock study of a weakly bonded layer structure: Brucite Mg(OH) 2, Phys. Rev. B. 47 (1993) 3522, https://doi.org/10.1103/PhysRevB.47.3522.
[31] D.E. Haycock, M. Kasrai, C.J. Nicholls, D.S. Urch, The electronic structure of magnesium hydroxide (brucite) using X-ray emission, X-ray photoelectron, and auger spectroscopy, J. Chem. Soc. Dalt. Trans. (1978) 1791–1796.
[32] M. B. Kruger, Q. Williams, R. Jeanloz, Vibrational spectra og Mg(OH)2 and Ca(OH) 2 under pressure, J. Chem. Phys. 91 (n.d.) 5910–5915.
[33] K.-H. Goh, T.-T. Lim, Z. Dong, Application of layered double hydroxides for removal of oxyanions: A review, Water Res. 42 (2008) 1343–1368, https://doi.org/10.1016/j.watres.2007.10.043.
[34] E. Makkos, A. Kerridge, J. Austin, N. Kaltsoyannis, Ionic adsorption on the brucite (0001) surface: A periodic electrostatic embedded cluster method study, J. Chem. Phys. 145 (2016), 204708, https://doi.org/10.1063/1.4968035.
[35] K.W. England, M.D. Parris, The Unexpected Rheological Behavior of Borate-Crosslinked Gels, Hydraul. Fract. Technol. Conf. (2011) SPE-140400-MS. doi: https://doi.org/10.2118/140400-MS.
[36] G. Hongchang Pang, W. Ning, J. Gong, Y. Lina Yea, Direct synthesis of hexagonal Mg(OH)2 nanoplates from natural brucite without dissolution procedure, Chem. Commun. 47 (2011) 6317–6319, https://doi.org/10.1039/C1CC10279F.